

Length-Scale of Glassy Polymer Plastic Flow: A Neutron Scattering Study

Frederic Casas,[†] Christiane Alba-Simionesco,[†] Helene Montes,^{*,‡} and François Lequeux[‡]

Université de Paris 11, Chimie Physique Laboratoire, UMR 8000, Bâtiment 349, F-91405 Orsay, France, and UMR 7615, ESPCI, 10 Rue Vauquelin, 75005 Paris

Received July 6, 2007; Revised Manuscript Received November 23, 2007

ABSTRACT: We aim to understand the effect of plastic deformation on the structure of a polymer glass. For that purpose, we measured by neutron scattering the structure of a polymethylmethacrylate (PMMA) sample stretched both below T_g ($T_g - 26$ K) and above T_g ($T_g + 30$ K) over a large length scale range. We observed that the plastic deformation is homogeneous at large length scales and it is affine at scales larger than around the half of the entanglement distance. Moreover at length scales about the monomer size, the structure of the stretched glassy polymer chains remains nearly isotropic but appears also slightly distorted by the plastic deformation. These distortions at the molecular scale are probably the mode of storage of internal energy for stretched glassy polymer.

1. Introduction

Contrary to molecular glasses, polymer glasses are able to submit to large deformations without fracture suggesting that the polymeric nature of the glass is of importance for plasticity. However, the intimate mechanisms of plasticity are still puzzling for the physicist. Their amorphous structure combined with their extremely slow spontaneous dynamics and their ability to sustain large deformations make glassy polymers fascinating objects.

Up to now two kinds of approaches have been considered for the plastic flow of glasses. The first approach is based on macroscopic experiments, mostly thermomechanic ones. The second approach relies on simulation of molecular glasses, probably because fractures can be avoided from simulations.

When submitted to a mechanical solicitation in the plastic regime, glassy polymers undergo rearrangements and consequent structural modifications.^{1–4} We can mention two of those effects. First, a plastic deformation induces local structural changes. For instance, the cold-drawn polymers exhibit a “larger mobility” than the nonstretched systems.^{5,6} Second, part of the mechanical work necessary for the plastic deformation is stored.^{1,2} This leads to an increase of the internal energy, that can be released into heat at a temperature higher than the cold-drawing one. Hence the thermodynamic state of cold-drawn polymers is very different from the one of unstrained glassy polymers. However, very few structural studies have been performed on plastified polymers. One of the classical pictures is that the plastic deformation induces the creation of “rubber-like” domains.^{3,4} Their size is around a few nanometers, and their density decreases during the plastic flow as observed by PALS⁷ and more recently by SAXS.⁸

Simulation of the flow of glasses is clearly a difficult task. The simulation can be performed for glasses at zero temperature but even so, this is not an easy task, as explained by Maloney and Lemaitre.⁹ Alternatively, it can be performed using molecular dynamics but thus is limited to systems very near the glass transition temperature T_g as it is up to now difficult to exceed the millisecond range for this type of simulation.

The simulations at zero temperature have shown that molecules rearrange in small domains, with irreversible motions. These localized plastic events appear to be strongly correlated in space,^{9,10} leading eventually to a self-organized critical arrangement.¹¹

Molecular dynamics of polymer glasses have shown that, on the contrary, the deformation is very similar to the one of a molten polymer due to the effects of the chain topology.^{21–24}

Here we investigate experimentally the consequence of a large plastic deformation on the structure of a polymer glass. Observations were performed over a huge range of length scales, using neutron scattering experiments. We aim to address the two following questions: at which length scale mechanical energy is stored and what is the length scale above which the deformation is homogeneous, i.e., affine.

2. Experimental Section

We performed neutron scattering experiments on a syndiotactic poly(methylmethacrylate) at various scales using two types of labeling. Measurements were performed using two kinds of scattering techniques: for the q values from 0.003 to 0.3 Å^{−1}, we used small angle neutron scattering spectrometers (KWS2 at IFF-Juelich and D22 at ILL-Grenoble). For larger q values from 0.5 to 10 Å^{−1}, measurements were carried out with two axis diffractometers (7C2 at LLB-Saclay and D16 at ILL-Grenoble).

As we aim to compare the structure of polymer chains stretched, respectively, below and above their glass transition temperature T_g , we choose to work with cross-linked PMMA chains. For large q vectors, $q > 1$ Å^{−1}, we used 100% cross-linked deuterated PMMA chains.

For smaller q vectors ($q < 1$ Å^{−1}) the samples provided by Polymer Source consisted of 10% long deuterated PMMA chains in a hydrogenated PMMA network. The deuterated chains have a molecular weight $M_w = 200\,000$ g/mol, that corresponds to about 20 M_e . The glass transition temperature, T_g , as determined by DSC at 10 K/min is 392 K.

Samples measured by SANS were prepared as following. Deuterated chains were first mixed with protonated methylmethacrylate monomers. Then the network of cross-linked protonated chains is built by UV irradiation. We chose diacrylate butanediol as the cross-linker. In order to initialize the polymerization and reticulation, we added a photoinitiator (Irgacure (Ciba, France)) (0.1 wt % monomer). The concentration of cross-linker

* Corresponding author. E-mail: helene.montes@espci.fr.

[†] Université de Paris 11.

[‡] UMR 7615, ESPCI.

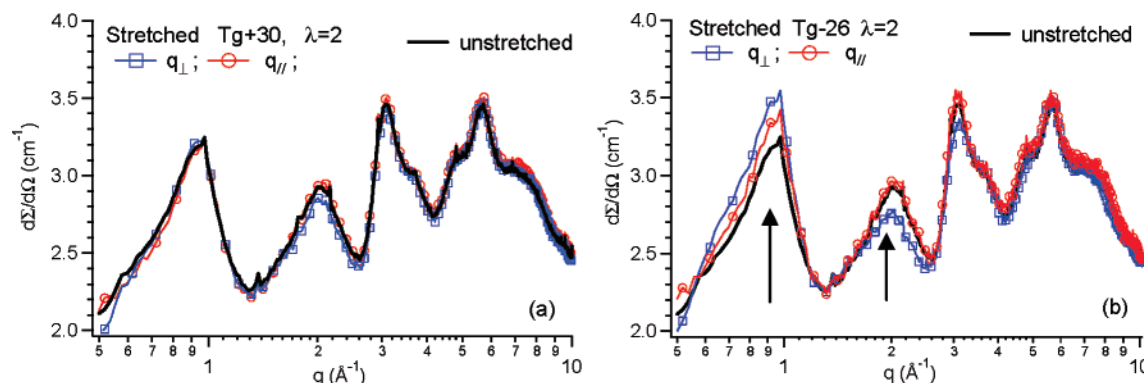


Figure 1. Local structure factor measured by neutron diffraction on stretched fully deuterated cross-linked PMMA chains ($\lambda = 2$). Measurements were performed parallel (q_{\parallel}) and perpendicular (q_{\perp}) to the stretching direction. (a) Structure factor measured on PMMA stretched above T_g . The scattered intensity of the sample stretched above the glass transition is equal to the one of the isotropic sample. (b) Structure factor measured on PMMA chains stretched below T_g . Except at the two peaks indicated by the arrows, there are no differences in this q range between the isotropic and the stretched samples.

was kept equal to 0.6% per mol of methylmethacrylate monomers such that the average weight between cross-links M_c was similar to the entanglement distance M_e . ($M_e \approx 9000$ g/mol for protonated chains and $M_e \approx 10\,000$ g/mol for fully deuterated chains corresponding to an entanglement length of about 60 \AA).

The whole deuterated samples were obtained by the polymerization and the reticulation of deuterated monomers. The same concentration of photoinitiator and cross-linker were used: 0.6% of diacrylate butanediol per mol of methylmethacrylate monomers and 0.1% weight of photoinitiator.

Using a Zwick apparatus, samples having a dog-bone shape were stretched at a given temperature chosen between $T_g - 28 \text{ K} = 363 \text{ K}$ to $T_g + 30 \text{ K} = 423 \text{ K}$. The samples were quenched to room-temperature, 293 K , just after the end of stretching.

In order to be able to detect by neutron scattering some significant effect of the stretching on the chains structure, polymer chains must have reached an extension of at least 150%. In this elongation range, polymer chains are clearly in the strain-hardening regime, far from the yield point located around an elongation rate $\lambda = 1.1$.¹

In order to avoid history effects and/or aging relaxations, neutron measurements were always performed on samples that were quenched and stored at room temperature. First DSC measurements have shown that cold-drawing erases the physical aging stored by the sample before stretching.^{1,12} Thus we are sure that the thermomechanical history of our samples before the plastic deformation do not have an effect on their structure after a stretching below T_g . Second, the samples after cold-drawing are kept at room-temperature. For a few days, there is not any relaxation at this temperature, namely, $T_g - 90 \text{ K}$. Thus, using this protocol we are sure to avoid the uncontrolled effect of slow relaxations on the structure.

3. Experimental Results

3.1. Effect of Stretching on the Chain Structure at Local Length Scales ($< 1 \text{ nm}$). In Figure 1, we have plotted for large q vectors the intensity scattered by a sample stretched above T_g (Figure 1a) and by a cold-drawn system (Figure 1b). We measured the structure factor both perpendicularly and parallel to the direction of the stretching. Data were compared to the ones obtained on an unstretched system.

For systems stretched above T_g (at $T = 420 \text{ K}$), the scattering is isotropic and exactly equal to the one of the unstretched samples. On the contrary, we observed a small anisotropy with the system stretched below T_g . The anisotropy is however weak and is localized on the two first peaks of the local structure factor, respectively, at $q = 0.9 \text{ \AA}^{-1}$ and $q = 2 \text{ \AA}^{-1}$. According to the simulation works of Genix et al.,¹³ the first peak at $q = 0.9 \text{ \AA}^{-1}$ is related to the interchain correlations. The peaks visible at large q values resulted from the intrachain correlations

existing between several atomic groups composing the monomer unit. In particular, the peak visible at 2 \AA^{-1} is due to the correlations between two ester groups. Stretching below T_g changes thus only slightly the correlation distances between the two main chains and between atomic sequences of neighboring monomer units.

At these length scales, polymer chains stretched below T_g are slightly distorted compared to isotropic samples or samples stretched above T_g .

3.2. Effect of Stretching on the Chain Structure at Large and Intermediate Length Scales. At smaller q vectors, the chain labeling we chose allows one to observe intrachain correlation of a single deuterated chain diluted into a matrix of cross-linked hydrogenated chains. The solid line of Figure 2 presents the intensity scattered by unstretched chains. The scattering behavior is classical and follows the Debye law. For $qR_g < 1$ (R_g being the gyration radius of the deuterated chains), the form factor reaches a plateau, while it decays with an exponent close to -2 for $qR_g > 1$.

In the following, we will compare the form factor of unstretched chains to the one of chains quenched immediately after stretching. We will only discuss the intensity scattered parallel and perpendicular to the stretching direction.

3.2.1. Structure of Chains Stretched above T_g . We measured the structure of chains stretched at $T_g + 30$ and quenched at room temperature ($T_g - 90$) immediately after stretching. In Figure 2a, we observe that the scattered intensity is anisotropic. In Figure 2, data measured parallel and perpendicular to the stretching are plotted as a \circ and \square , respectively.

If the affine assumption is valid, scattered intensity measured on the stretched samples should superimpose onto the one obtained on the nondeformed system by taking into account the deformation undergone by the radius of gyration after stretching. On Figure 2b we have plotted the data measured perpendicular and parallel to the stretching direction as a function of the reduced wavevectors q_{\perp}^* and q_{\parallel}^* , respectively. q_{\perp}^* and q_{\parallel}^* are defined by: $q_{\perp}^* = q/\sqrt{\lambda}$ and $q_{\parallel}^* = q\lambda$.

We observe that at small q values, $q < 0.04 \text{ \AA}^{-1}$, data collected on the stretched sample superimpose the ones of the isotropic sample in reduced q -vector units. This experimental result indicates that the deformation is affine at the large length scale. However at large q values, $q > 0.04 \text{ \AA}^{-1}$, the superposition fails meaning that, at the corresponding smaller length scales, local deformation deviates from the macroscopic one. The crossover wave vector between the affine and nonaffine regime will be called q_c^* (see Figure 2).

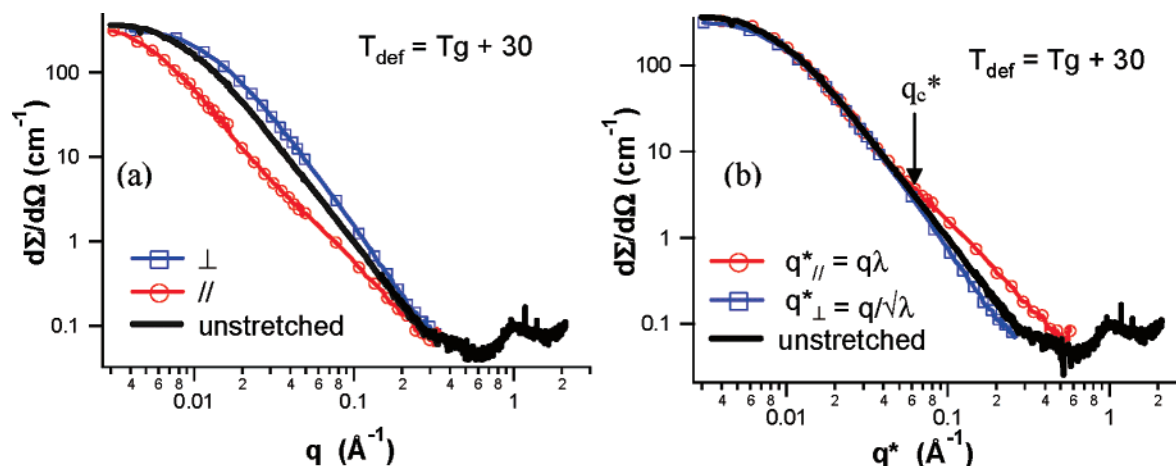


Figure 2. (a) Intensity scattered of a sample stretched above T_g compared to the unstretched sample. Measurements were performed on a sample composed by 90% of cross-linked hydrogenated chains mixed to 10% of deuterated chains. $d\epsilon/dt = 1 \text{ s}^{-1}$; $\lambda = 1.7$. (b) Scattered intensity in reduced q -vector. Deviation from an affine deformation clearly appears for large q -vectors.

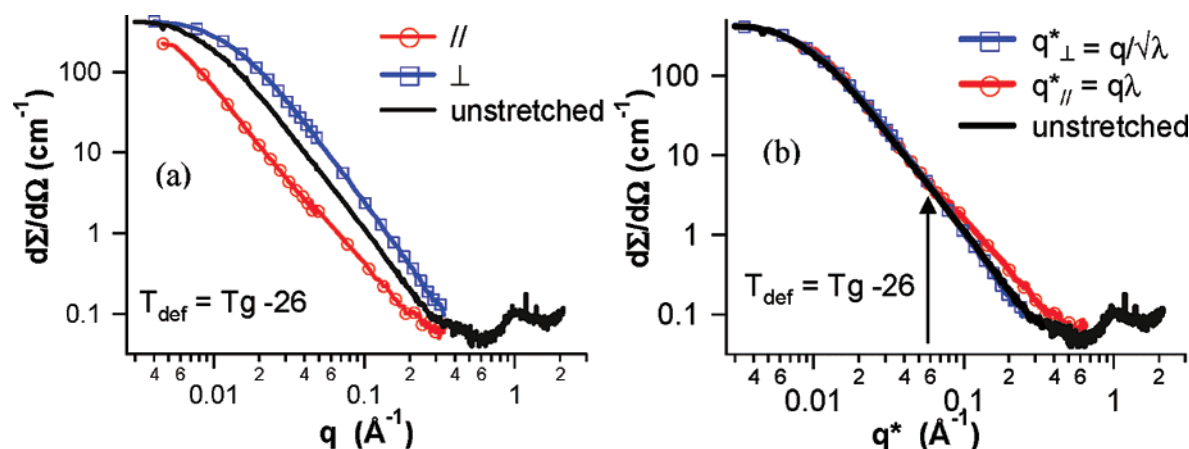


Figure 3. (a) Scattered intensity of a cold-drawn sample compared to the one of an unstretched sample. Measurements were performed on a sample composed by 90% of cross-linked hydrogenated chains mixed to 10% of deuterated chains. $d\epsilon/dt = 0.001 \text{ s}^{-1}$. $\lambda = 1.8$. (b) Scattered intensity in reduced q -vector. Deviation from the affine motion clearly appears for large q -vectors.

Similar results were observed on polymer melts stretched above T_g ^{15–19} and kept at the temperature of the stretching during a given rest time. These previous works showed that the deviation from affine deformation originates in the partial relaxation of the chains occurring when the experiment times are of the order of the chain relaxation times. In this case, chain relaxation starts from the small length scale and propagates toward the larger one.¹⁵ These studies showed that the value of the crossover wave vector q_c^* depends thus on the time elapsed between the end of the deformation and the observation of the chain structure. For increasing rest time, the crossover between affine and nonaffine domains just shifts toward larger and larger length scale (small q). If chains are not cross-linked, they go back to an isotropic conformation after a required rest time, typically the reptation time. In this case, the whole relaxed chain structure is not affine at all but equal to the one of a nonstretched sample.

If the chains are cross-linked, they cannot relax completely, and thus an affine deformation is only observed at large scale while the structure at smaller scales (large q) is fairly complex leading to the famous “butterfly” patterns.^{16–19}

In our experiment, samples were quenched immediately at the end of stretching. However, the relaxation times of the chains at $T_g + 30$ are on the order of the stretching times, i.e., a few seconds. For instance, the relaxation time of a chain segment of length M_e , about 60 Å for PMMA chains, is around $\tau_e =$

0.1 s. This time τ_e is short compared to the reptation time of the deuterated chains ($\tau_{\text{rep}} = 2000 \text{ s}$). The experimental time is thus large compared to the relaxation times involved at the small length scale. This explained why the intensity scattered by the stretched sample is isotropic at $q > 0.2 \text{ Å}^{-1}$ (see Figure 2a): the chains have already relaxed their deformation at the small length scale. This feature is also consistent with observations made at even smaller length scales ($< 1 \text{ nm}$) shown on Figure 1a. Finally, the crossover length ($1/q_c^*$) we observed after stretching above T_g defines the length scale above which there were no longer structural relaxations toward isotropic conformations after stretching.

3.2.2. Structure of Chains Stretched Below T_g . We studied the structure of chains that were immediately quenched at $T_g - 90$ after a stretching performed at $T_g - 30$. In the glassy state, the chain dynamics is extremely slow. For instance at $T = 363 \text{ K} = T_g - 30 \text{ K}$, the value of the reptation time τ_{rep} can be estimated at 10^{20} s and the time of α -like rearrangements is of the order of 10^{14} s . In this temperature range, the relaxation times are very large compared to the time involved in the experiment (the time needed for the cold-drawing, 10^5 s and time of quench). Thus we do not expect any partial chain relaxation at small length scales during the quench from $T_g - 30$ to $T_g - 90$ or after the quench. At $T_g - 90$, segmental rearrangements associated to physical aging should be negligible.

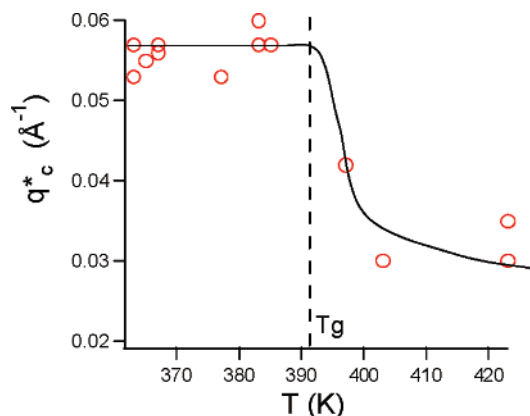


Figure 4. Variation of q_c^* versus temperature of stretching.

Figure 3a shows the raw results obtained on polymer chains stretched below T_g while Figure 3b presents the data plotted versus the reduced variables q_{\perp}^* and q_{\parallel}^* .

As seen in Figure 3b, we observed that at small q values, the deformation appears to be affine as was the case for samples stretched above T_g .

However, for q values larger than 0.06 \AA^{-1} , a deviation from affine deformation was observed in the direction parallel to the stretching direction. On the other hand, we did not observe any significant deviation from affinity perpendicular to it. Our observations agreed with the results previously obtained by Dettenmaier on noncross-linked cold-drawn PMMA chains in the q -window $0.001\text{--}0.6 \text{ \AA}^{-1}$.¹⁴

Finally we can see on Figure 3a, that the scattered intensity tended to recover the value of the isotropic one at a large q value, $q \approx 0.3 \text{ \AA}^{-1}$. This last feature was coherent with the observations made at larger q values, $q > 0.5 \text{ \AA}^{-1}$, presented in Figure 1b which revealed a nearly isotropic structure at a very local length scale.

We measured the value of q_c^* on samples stretched below T_g at different temperatures and different stretching rates. We did not observe any significant dependence of q_c^* neither versus deformation rate nor versus temperature. On the contrary, above T_g , the value of q_c^* was governed by the relaxation times of the polymer chains. q_c^* variations are summarized in Figure 4.

4. Discussion

We measured by neutron scattering the structure of free entangled PMMA polymer chains ($M_w = 20 M_e$) inserted in a network of cross-linked PMMA chains. Observations were made on systems having undergone a large deformation ($\lambda \approx 2$) below T_g . In this deformation range, the polymer chains were in the strain-hardening regime as is visible on Figure 5. Our measurements are performed in the stress-strain range where the true strain σ_{true} varies linearly with $(\lambda^2 - 1/\lambda)$.

This variation in $(\lambda^2 - 1/\lambda)$ is reminiscent of the deformation of an elastomer network and is a signature of the topological mechanism involved in the plastic deformation. The variation of stress with strain in our experiments can be described using the Gaussian strain-hardening phenomenological model²⁰ that writes

$$\sigma_{\text{true}} = \sigma_0 + G_R(\lambda^2 - 1/\lambda)$$

This model assumes that the chains keep their Gaussian statistics. G_R , called the hardening modulus, is the modulus of the polymer network stretched below T_g .

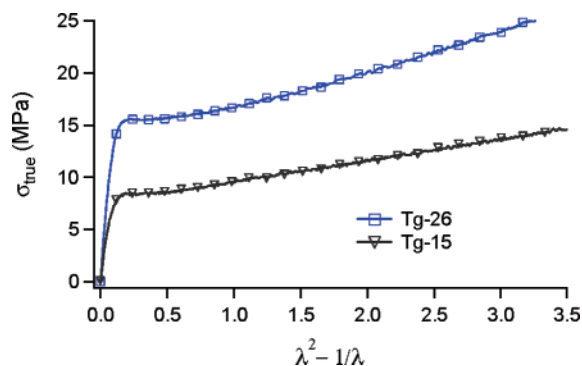


Figure 5. Variation of the true stress σ_{true} versus $(\lambda^2 - 1/\lambda)$ for cold-drawn samples studied with neutron scattering.

Such stress-strain behavior is commonly observed on many polymer glasses. Recently, measurements by solid-state NMR of segmental orientation in plastically deformed glassy polymers^{21,22} indicated that orientation-strain relationships of chain segments agree below T_g with predictions from the rubber-elastic affine network model. This confirms the fact that the variation in $(\lambda^2 - 1/\lambda)$ originates from the topology of a polymer network that we will call the “glassy apparent network” as it will appear to be different from the usual network.

In fact, the precise nature of the topological constraints acting during strain hardening is still unknown. According to many mechanical experiments, it seems that the polymer network involved in the deformation of a polymer glass is related to the “classical” topological constraints such as entanglements and cross-links. For instance, the hardening modulus G_R increases as the density of entanglements or cross-links increases.²³ However, G_R has a different temperature dependence than the elastic modulus of an elastomer network. Moreover, G_R is much larger than the modulus value predicted by the entanglement or cross-links density according to a rubber elasticity model.

According to solid-state NMR experiments²² on plastically stretched glassy PMMA, the mesh size of the “glassy apparent network” could be fairly smaller than the entanglement distance and independent of cross-links or entanglement density. This feature agrees with numerical simulations²⁴ predicting strain-hardening for chains shorter than the entanglement length. However, this observation is not common to all polymer glasses. Similar NMR experiments performed on entangled polycarbonate chains led to the conclusion that the mesh size of the polymer network deformed below T_g is similar to the entanglement distance.²¹ Therefore, there must also be the complex effect of chain flexibility on the structure of polymer chains stretched below T_g .

Let us discuss now the results obtained by Hoy and Robbins²⁴ with simulations performed on entangled polymer chains compressed below T_g . For long entangled chains ($M_w > 10 M_e$), Hoy and Robbins observed an affine deformation at the end-to-end distance length scale. However at the scale of the monomer, nonaffine behavior is observed. At small deformations, this deviation from affinity does not depend on the topological constraints fixed by entanglements. According to their result, local rearrangements would involve chain segments smaller than M_e . However the deviations from affinity are enhanced by topological constraints in the strain-hardening regime, as revealed by the fact that the amplitude of these deviations increases with entanglement density.

To resume, their simulations show that the deformation in the strain-hardening regime is due to local plastic events involving local motions. Their number increases with topological

constraint density. The successive plastic rearrangements occur following the tension undergone locally by chain segments that is controlled by the topological constraints.

Thus both NMR and simulation show that the deformation of a glassy polymer is reminiscent from the one of an elastomer, stretched above its glass transition. The plastic events propagates in the sample following the topological constraint of a “glassy equivalent network”. The apparent mesh size of this “glassy equivalent network” is smaller than the one of the elastomer network.

In our work, we probed at several length scales the structure of glassy chains deformed in the strain-hardening regime. Our neutron scattering experiments performed over a large range of wave vectors, $0.003 \text{ \AA}^{-1} < q < 10 \text{ \AA}^{-1}$, reveals three main features: (i) cold-drawing induced a chain distortion at small length scales ($< 1 \text{ nm}$). It led to slight changes of the structure factor measured at very large q values (cf. Figure 1a); (ii) at scales larger than the mesh size, the chain deformation is affine; (iii) at intermediate length scales, smaller than M_e , the deformation is not affine anymore. It is especially visible in the direction parallel to the stretching. This deviation from affinity is different in nature to the one observed on polymer chains stretched above their T_g . At high temperature, the relaxation times of the polymer chains are indeed shorter than the typical times for the experiment, and thus polymer chains can then partially relax their deformation. The relaxation toward the unstretched coil conformation propagates from small to large length scales.

When stretching is performed below T_g , the relaxation times of the chains are very large, $\tau_\alpha = 10^{14} \text{ s}$, compared to the experiment duration, 10^5 s . Deviation from affine deformation observed on polymer chains stretched below T_g are thus due to relaxation mechanisms that are plastic in nature.

As a preliminary conclusion, we see that the deformation is affine for the large length scale, in agreement with the previous quoted idea of a “topological” network driving the polymer motion in the glassy state. We see also that the crossover between affine and nonaffine deformation is in the glassy state at a length scale about half of the one of the network involved in the molten state. This is also consistent with literature, simulation and NMR,²² even if the ratio of the two crossover lengths is smaller than the one seen by NMR.

Indeed like Wendlandt et al., we find that q_c^* does not depend on the strain rate applied to deform the glassy polymer, but the values of q_c^* indicate that the apparent mesh size of the glassy equivalent polymer network would be half of the entanglement distance. This size is quite larger than the one estimated by Wendland et al.²² who found a mesh size 6 times smaller than the entanglement distance. This could result from the two different geometries chosen to deform the glassy PMMA chains. We measured the structure of chains having undergone a tensile deformation which induces a strong chain alignment while the results of Wendland are observed on compressed samples that are more weakly oriented. Moreover, our experiments show that the local structure of the polymer after plastic deformation is not exactly the one of the same sample stretched above T_g . This feature has not been seen and taken into account neither by NMR nor in simulation.

More precisely at the very small scales, $1\text{--}10 \text{ \AA}^{-1}$, the local rearrangements involve chain distortions that modify the local chain structure factor that we observed for very large q values (cf. Figure 1b). These local plastic events favor the high-energy conformations leading to an increase of the internal energy of the glassy polymer. Part of the mechanical energy stored during cold-drawing is thus stored at a very small length scale. In

addition, we have observed that in the perpendicular direction, the deformation is nearly affine up to larger value of q^* than in the parallel direction. We suggest here that this could also originate from topological constraints. In fact the extensibility limit is reached in extension and thus in the stretching direction, the parallel direction in our case. Thus deviations from affine deformation are induced by part of the chains which are extended up to their limit, thus orientated parallel, but not perpendicular to the elongation axis. Thus the fact that the deformation seems more affine in the perpendicular direction than in the parallel one confirms the topological origin of the deformation field at the scale of the entanglements. This experimental observation is not observed on the polymer stretched above T_g . This feature indicates that the deformation of a polymer glass is more complex than that predicted by a rubber affine deformation model.

Last let us come back to the difference between the plasticity of molecular versus polymer glasses. Compared to what is observed in molecular glasses, the value of q_c^* found in our neutron experiments is quite large meaning that the deformation is affine until quite small length scales. This result could be understood if we take into account that there are in polymer glasses topological constraints that do not exist in molecular glasses. This is in our opinion a complementary signature that the number and spatial location of local plastic events are mainly controlled by the topological constraints existing in the system. The topological constraints govern homogeneous distribution within the sample while, on the contrary, in nonpolymeric glass, stress redistribution leads to very heterogeneous deformation.

5. Conclusion

We observed that cold-drawn polymer glasses exhibit affine deformation at large length scale. Below a typical length scale of the order of a few nanometers, there is a crossover regime toward a nearly isotropic structure. At the small scale, the polymer remains isotropic and slightly distorted. These distortions at the molecular scale are probably the mode of storage of internal energy for the glassy polymer.

The crossover length between the affine and nonaffine domain does not depend on strain-rate nor on temperature. Furthermore, it levels off at a length scale about the entanglement length. According to recent simulations made by Hoy and Robbins, we suggest that this length scale originates from topological constraints that induce very homogeneous deformation. Let us recall that on the contrary for nonpolymeric molecular glasses, the flow tends to be very heterogeneous. The role of topological constraint, and thus of the limit extensibility of the chains, was also exemplified by the fact that the deformation was affine up to scales smaller in the direction perpendicular to the extension than in the parallel one.

Acknowledgment. The authors acknowledge M. Robbins (John Hopkins University, Baltimore) for very fruitful discussions at the meeting of Les Houches on the “Flow of glassy systems” in February 2007.

References and Notes

- (1) Hasan, O. A.; Boyce, M. C. *Polymer* **1993**, *34*, 5085–5092.
- (2) Salamatina, O. B.; Rudnev, S. N.; Voenniy, V. V.; Oleinik, E. F. *J. Therm. Anal.* **1992**, *38*, 1271–1281.
- (3) Oleynik, E. *Prog. Colloid Polym. Sci.* **1989**, *80*, 140–150.
- (4) Oleinik, E. F.; Salamatina, O. B.; Rudnev, S. N.; Shenogin, S. V. *Polym. Sci.* **1993**, *35* (11), 1532–1558.
- (5) Trznadel, M.; Pakula, T.; Kryszewski, M. *Polymer* **1998**, *29*, 619–625.

- (6) Nanzai, Y.; Miwa, A.; Cui, S. Z. *JSME Int. J., Ser. A* **1999**, *42*, 479–484.
- (7) Hasan, O. A.; Boyce, M. C.; Li, X. S.; Berko, S. *J. Polym. Sci., Part B* **1993**, *31*, 185–197.
- (8) Munch, E.; Pelletier, J. M.; Vigier, G. *Phys. Rev. Lett.* **2006**, *97*, 207801–207804.
- (9) Maloney, C. E.; Lemaitre, A. *Phys. Rev. E* **2006**, *74* (1), Article No. 016118.
- (10) Picard, G.; Ajdari, A.; Lequeux, F.; Bocquet, L. *Phys. Rev. E* **2005**, *71*, 010501(R).
- (11) Chen, K.; Bak, P.; Obukhov, S. *Phys. Rev. A* **1991**, *43*, 625–630.
- (12) Casas, F.; Alba-Simionesco, C.; Lequeux, F.; Montes, H. *J. Non-Cryst. Solids* **2006**, *352* (42–45), 5076–5080.
- (13) Genix, A. C.; Arbe, A.; Alvarez, F.; Colmenero, J.; Schweika, W.; Richter, D. *Macromolecules* **2006**, *39*, 3947–3958.
- (14) Dettenmaier, M.; Maconnachie, A.; Higgins, J. S.; Kausch, H. H.; Nguyen, T. Q. *Macromolecules* **1986**, *19*, 773–784.
- (15) Blanchard Ariane SANS Study of the Non-Linear Relaxation Mechanisms in a Step-Strain Elongated Linear Polymer Melt. Ph.D. Dissertation, IFF, Germany, 2004.
- (16) Benoit, et al. *J. Polym. Sci., Polym. Phys. Ed.* **1976**, *14*, 2119–2128.
- (17) Ramzi, A.; Zielinski, F.; Bastide, J.; Boue, F. *Macromolecules* **1995**, *28*, 3570–3587.
- (18) Ramzi, A.; Hakiki, A.; Bastide, J.; Boue, F. *Macromolecules* **1997**, *30*, 2963–2977.
- (19) Zielinski, F.; Buzier, M.; Lartigue, C.; Bastide, J.; Boue, F. *Prog. Colloid Polym. Sci.* **1992**, *90*, 115–130.
- (20) Haward, R. N.; Young, R. J. *The Physics of Glassy Polymers*, 2nd ed; Chapman and Hall: London, U.K., 1997.
- (21) Utz, M.; Atallah, A. S.; Robyr, P.; Widmann, A. H.; Ernts, R. R.; Suter, U. W. *Macromolecules* **1999**, *32*, 6191–6205.
- (22) Wendlandt, M.; Tervoort, T. A.; Van Beek, J. D.; Suter, U. W.; Mech, J. *Phys. Solids* **2006**, *54*, 589–610.
- (23) Van Melick, H. G. H.; Govaert, L. E.; Meijer, H. E. H. *Polymer* **2003**, *44*, 2493–2502.
- (24) Hoy, R.; Robbins, M. *J. Polym. Sci.* **2006**, *44*, 3487–3500.

MA0714969